HHS Public Access

Author manuscript

Clin Pharmacol Ther. Author manuscript; available in PMC 2019 February 01.

Published in final edited form as:

Clin Pharmacol Ther. 2018 February ; 103(2): 332–340. doi:10.1002/cpt.742.

A primary human lung alveolus-on-a-chip model of intravascular thrombosis for assessment of therapeutics

Abhishek Jain[1,2,3,¶,†], **Riccardo Barrile**[1,Ω,†], **Andries D. van der Meer**[1,§], **Akiko Mammoto**[2], **Tadanori Mammoto**[2], **Karen De Ceunynck**[3], **Omozuanvbo Aisiku**[3], **Monicah A. Otieno**[4], **Calvert S. Louden**[4], **Geraldine A. Hamilton**[5], **Robert Flaumenhaft**[3], and **Donald E. Ingber**[1,2,6,*]

[1]Wyss Institute for Biologically Inspired Engineering, Harvard University, Boston, MA 02115, USA

[2]Vascular Biology Program and Department of Surgery, Boston Children's Hospital and Harvard Medical School, Boston 02115, USA

[3]Division of Hemostasis and Thrombosis, Department of Medicine, Beth Israel Deaconess Medical Center, Harvard Medical School, Boston, MA 02115, USA

[4]Janssen Pharmaceutical Research and Development, Pre-Clinical Development and Safety, 1400 Welsh and McKean Road, Spring House PA 19477

[5]Emulate Inc., 27 Drydock Avenue, Boston, MA 02210, USA

[6]Harvard John A. Paulson School of Engineering and Applied Sciences, Cambridge, MA 02138, USA

Abstract

Pulmonary thrombosis is a significant cause of patient mortality, however, there are no effective *in vitro* models of thrombi formation in human lung microvessels, that could also assess therapeutics and toxicology of antithrombotic drugs. Here we show that a microfluidic lung alveolus-on-a-chip lined by human primary alveolar epithelium interfaced with endothelium, and cultured under flowing whole blood can be used to perform quantitative analysis of organ-level contributions to inflammation-induced thrombosis. This microfluidic chip recapitulates *in vivo* responses, including platelet-endothelial dynamics and revealed that lipopolysaccharide (LPS) endotoxin indirectly stimulates intravascular thrombosis by activating the alveolar epithelium, rather than

[*]Address all correspondence to: Donald E. Ingber, M.D., Ph.D., Wyss Institute at Harvard University, 3 Blackfan Circle, CLSB 5, Boston, MA 02115 (don.ingber@wyss.harvard.edu; tel: 617-432-7044; fax: 617-432-7068).

[¶]Present Address: Department of Biomedical Engineering, Dwight Look College of Engineering, Texas A&M University, College Station, TX

[Ω]Present address: Cedars-Sinai Medical Center, Los Angeles, CA

[§]Present address: MIRA Institute for Biomedical Technology and Technical Medicine, University of Twente, Enschede, The Netherlands

[†]These authors contributed equally

CONFLICT OF INTEREST DISCLOSURE: D.E.I and G.A.H. are founders, and hold equity in Emulate, Inc. and D.E.I. chairs it scientific advisory board; A.D.v.d.M serves as a scientific consultant to the company.

AUTHOR CONTRIBUTIONS:

D.E.I., A.J., and R.B. wrote the manuscript; D.E.I., A.J., R.B., A.D.v.d.M., K.D.C., and R.F. designed the research; A.J., R.B., A.D.v.d.M., A.M., T.M., and K.D.C. performed the research; D.E.I., A.J., R.B., K.D.C., M.A.O., C.S.L., and G.A.H. analyzed the data; A.M., T.M., K.D.C., and O.A. contributed new reagents/analytical tools.

acting directly on endothelium. This model is also used to analyze inhibition of endothelial activation and thrombosis due to a protease activated receptor-1 (PAR-1) antagonist, demonstrating its ability to dissect complex responses and identify antithrombotic therapeutics. Thus, this methodology offers a new approach to study human pathophysiology of pulmonary thrombosis and advance drug development.

INTRODUCTION

Thrombi that form within lung vessels due to activation of platelets and inflammatory stimulation of the pulmonary vascular endothelium are a major cause of patient mortality and morbidity in many lung diseases, including acute lung injury [1–5]. Intense basic research efforts have provided new biological insights into the pathology of pulmonary thrombosis [2,4,6]; however, development of new therapies that target thromboinflammatory mechanisms has been hampered by the lack of models and methods that permit analysis of the organ-level responses that underlie this lung condition in humans. Animal models of pulmonary microvascular thrombosis exist, but they do not mimic the altered hemostasis and hemodynamic complexity of human lung [7,8]. With animal models, it is also not possible to separate contributions of platelet-endothelial interactions versus tissue-tissue (e.g., epithelial-endothelial) interactions that can contribute to development of thrombotic lesions in response to epithelial injury or inflammation induced by chemicals or mechanical injury [9,10]. In addition, there is a critical need to develop *in vitro* disease models that can more effectively predict responses in humans because of ethical issues associated with animal testing [11,12]. Although there are existing *in vitro* coagulation and platelet function assays, they do not incorporate physiological organ-level signaling between endothelial and parenchymal tissues, inflammatory activities, or relevant fluid hemodynamics which are all key determinants of thrombosis [13–18]. Due to these existing deficiencies, we explored whether microfluidic organ-on-a-chip (organ chip) technology [12,19] can be used to address this challenge.

Human organs chips are microfluidic culture systems created with microchip manufacturing methods that contain hollow microchannels lined by living human cells that recapitulate organ-specific tissue-tissue interfaces and physical microenvironments (including fluid flow, air-liquid interfaces, and cyclic deformation in the case of the lung) that are necessary to mimic human organ level pathophysiology [12]. Here, we significantly modified a previously described human lung chip [20,21] by replacing the established lung alveolar epithelial cell line (A549) originally isolated from a lung tumor [22] with primary human lung alveolar epithelial cells. We also lined all four walls of the second microchannel with human vascular endothelial cells to form a continuous endothelium-lined tube that enables human whole blood to be perfused through the chip instead of culture medium. This new primary human lung alveolus chip design enables whole human blood to be perfused through the vascular channel without producing thrombus formation under control conditions, while allowing high resolution, real-time analysis of interactions between human blood cells and endothelial cells in an organ-relevant context. Using this technology in combination with novel analytical tools for quantitation of dynamic platelet-endothelial interactions and clot formation, we demonstrate a key role of the epithelium in inflammation-driven vascular

thrombosis during lipopolysaccharide endotoxin (LPS)-induced acute lung injury, and show that the model can be used to evaluate cytoprotective effects of a potential therapeutic with anti-thrombotic and anti-inflammatory activities *in vitro*.

RESULTS

Primary human lung alveolus chip

To develop an organ-level model of vascular inflammation-induced human pulmonary thrombosis *in vitro* that is also capable of dissection of intercellular communication, we modified a previously described lung chip microfluidic device that consists of two parallel rectangular microchannels separated by a thin, porous, flexible membrane coated with extracellular matrix (ECM) [20,21,23]. First, we increased the microchannel dimensions of both the chambers in order to maximize the surface area exposed to blood and soluble factors. Then we covered all surfaces of the bottom microchannel with human umbilical vascular endothelial cells (HUVECs) in order to engineer a three dimensional (3D) microvessel that prevents contact of blood with the surrounding pro-thrombotic ECM-lined channel walls as occurs in living vessels (Fig. 1a–c; **see METHODS for details**). Finally, primary human alveolar (mixture of type I and II) epithelial cells were cultured on the upper surface of the ECM-coated porous membrane instead of cells of an established, tumor-derived lung epithelial cell line as used in past lung chip studies. Using this new method, we were able to recreate a 3D cross-section of a human lung alveolus composed of an alveolar-capillary interface and a vascular lumen through which human whole blood can be perfused (Fig. 1c and Fig. S1). This improved lung alveolus chip maintained a viable epithelial-endothelial interface for more than 12 days under laminar flow (Fig. 1d–f), with both layers lined by cells joined via continuous intact cell-cell junctions lined by ZO-1 in the epithelium (Fig. 1d) and VE-cadherin in the endothelium (Fig. 1e, Movie 1).

Dynamic quantitative analysis of pulmonary thrombus formation in vitro

Before we initiated studies at the organ-level with the lung alveolus chip, we performed experiments to confirm that the engineered endothelium-lined tube within the lower vascular channel can be used to quantify thrombus formation under fluid shear conditions *in vitro*. As a positive control, we first perfused re-calcified (coagulation-activated) citrated human whole blood (shear stress: 3 N m^{-2}) containing fluorescently-labeled platelets through a collagen-coated lower microchannel that did not have an endothelial cell lining. As expected [24,25], collagen exposure led to rapid platelet adhesion to the walls of the microchannel within minutes (Fig. 2a, top; Movie 2), similarly to what is observed during hemostatic plug formation induced by vascular injury *in vivo* [26]. In contrast, when endothelial cells were cultured on all the surfaces of all four walls of the ECM-coated microchannel to form a hollow microvessel lined by a continuous vascular endothelium (Fig. 1f and Fig. S1) and human whole blood was perfused through its lumen for 20 minutes, both platelet adhesion and thrombi formation were completely prevented in this healthy engineered microvessel (Fig. 2a, middle; Movie 3). However, when the endothelium was stimulated with the inflammatory cytokine, tumour necrosis factor-α (TNF-α; 100 ng mL^{-1}) prior to initiating blood flow, the inflamed vascular endothelium promoted rapid

platelet recruitment and thrombus formation (Fig. 2a, bottom; Movie 4), as occurs within inflamed microvessels *in vivo* [27,28].

Interestingly, in contrast to the distributed fibrillar pattern of platelet-rich thrombi formed on the exposed collagen surface (Fig. 2a, top), the thrombi formed on the inflamed endothelium exhibited a distinct tear drop-like morphology (Fig. 2a, bottom right). While this unique thrombus morphology has not been observed in previous *in vitro* platelet adhesion studies that used collagen-coated microfluidic chambers [24,25], platelet aggregates have been reported to progressively grow and move downstream along the endothelial surface under flow *in vivo* [29–31]. Indeed, we could detect that this type of dynamic platelet-endothelium binding behaviour is responsible for this tear drop morphology when we performed video microscopic analysis of thrombi formation in the endothelium-lined vascular channel (Movie 2–4). Moreover, we observed formation of thrombi with a nearly identical tear drop shape and similar rapid platelet binding dynamics when we analyzed thrombi formation *in vivo* (Fig. 2b and Movie 5) in a previously described living mouse model of laser-induced thrombosis [30,32]. Thus, these initial studies suggest that the engineered microvessel within this microfluidic chip appears to recapitulate the unique shape and platelet dynamics associated with thrombus formation *in vivo*, whereas this is not observed in ECM-coated microfluidic devices that are commonly used for *in vitro* analysis of thrombus formation under flow [33].

To quantify these dynamic binding interactions between platelets and endothelium, we applied a recently developed automated imaging program [28] in order to measure the kinetics of platelet binding along the length of the microfluidic channel, and we derived a non-dimensional statistical method to arrive at a novel quantitative index of platelet binding dynamics (PBD index; Fig S2; **see METHODS for details**). When we calculated the PBD index for platelet interactions measured on collagen under flow, we found it to be extremely low because once the platelets adhere, they do not change their position (Fig. 2c, top and Fig. 2d). In contrast, when we stimulated the endothelium in the microchannel with increasing doses of TNF-α that induce a dose-dependent increase in expression of the surface adhesion molecule ICAM-1 (Fig. 2e), we observed a corresponding dose-dependent rise in both platelet binding to the endothelium (Fig. 2c) and in the PBD index (Fig. 2d), confirming the sensitivity of this method to detect dynamic thromboinflammatory interactions between platelets and endothelium associated with vascular inflammation. Moreover, this dynamic analytical method can distinguish platelet accumulation due to vascular injury (ECM exposure) in a healthy endothelium compared to thrombosis caused by endothelial activation by inflammatory stimuli, whereas quantitation of the average area of platelet adhesion (percentage platelet coverage relative to total area of channel) frequently used to analyse thrombosis on exposed ECM-coated substrates *in vitro* [25] cannot (Fig. S3). Additionally, we found that this PBD index increased when we raised the hemodynamic shear rate from 275 s^{-1} to 750 s^{-1} in the microfluidic channel (by altering pumping rates), indicating a higher tendency to form platelet-rich thrombi and promote platelet-endothelial binding interactions *in vitro* (Fig. 2d), as reported in past studies [34,35]. In contrast, quantification of the average area of platelet adhesion [24,25] was not sensitive to this change in shear (Fig. S3). Finally, we used the same method to analyse a single thrombus formed in

a laser-injured mouse vessel to confirm the relevance of the PBD index in a physiologically-relevant *in vivo* model of thrombosis. Again, using the same analytical method in combination with pseudo-colouring of images to indicate the local PBD index, we confirmed that the dynamics of platelet-endothelial binding were more rapid along the boundary of the thrombus compared to its central core (Fig. 2f, left), and we observed a pattern of platelet-endothelial binding dynamics within individual thrombi that was nearly identical to that seen within thrombi that formed in our endothelium-lined microfluidic channel *in vitro* (Fig. 2f, right). These regional heterogeneities in thrombus dynamics have been shown to be due to the thrombus consisting of a stable core region surrounded by reactive unstable shell [31,36], but to our knowledge, they have not been previously shown in cultured living endothelium or characterized *in vitro*.

Inflammatory cytokine-induced pulmonary thrombosis in the human lung alveolus chip

We then explored whether we could study organ-level contributions (as opposed to endothelial tissue-level contributions alone as done above) to vascular inflammation-driven thrombus formation using the human lung alveolus chip that contains human primary alveolar epithelium on the top of the ECM-coated membrane, closely interfaced with the human endothelium-lined vascular channel below (Fig. 1). When we perfused fluorescent tracer dye (4 kDa dextran) through the vascular channel of alveolus chip cultured for 12 days, we found that the alveolar-capillary interface formed on-chip retained a high level of pulmonary barrier function with low permeability to the dye (Fig. 3a), confirming past results using lung chips lined by an established human A549 alveolar cell line [20,21]. Importantly, we also were able to perfuse recalcified, citrated human whole blood for up to 20 minutes (shear rate: 275 sec^{-1}) through the vascular lumen of the lung alveolus chip without producing any significant platelet adhesion or blood clotting (Movie 6), as observed using a microfluidic system lined only by endothelium (Fig. 2a, middle; Movie 2). Direct addition of increasing doses of TNF-α to the alveolar epithelium compartment resulted in a dose-dependent increase in pulmonary vascular permeability (Fig. 3a) as well as a concomitant increase in ICAM-1 expression on the endothelium below (Fig. 3b). As expected, induction of ICAM-1 expression on the endothelium by delivery of TNF-α into the epithelial compartment of this organ-level model of an inflamed endothelium was accompanied by a dose-dependent increase in platelet-endothelial binding dynamics (Fig. 3c), as previously observed when TNF-α was infused directly through the endothelium-lined vascular channel (Fig. 2d). Thrombi formed over the entire endothelial surface within the vascular compartment of the lung alveolus chip, and they contained both platelets and fibrin by the end of the assay (Fig. 3d). Thus, this microfluidic system can effectively model the pro-inflammatory effects of TNF-α released into the epithelial compartment that lead to activation of the underlying endothelium and subsequent induction of intravascular blood thrombus formation.

LPS-induced pulmonary thrombosis is mediated by activation of the epithelium

Then we tested the effects of LPS on vascular thrombus formation using the pulmonary alveolus chip because this Gram negative bacterial endotoxin has been shown to cause acute lung injury and induce pulmonary thrombosis *in vivo* [37,38]. When we first added LPS (100 ng mL^{-1}) directly to medium flowing through the vascular channel lined by the endothelial

tissue (in the absence of the alveolar epithelium) for 2 hours, we could not detect any significant change in barrier permeability (Fig. 4a), endothelial junctional integrity (Fig. 4b,c) or ICAM-1 staining (Fig. 4d) compared to untreated organ chips. Thus, LPS does not exhibit its reported ability to induce pulmonary thrombosis when analyzed at the tissue level alone (i.e., using only vascular endothelium under flow) at the dosage and time that we applied. In contrast, we observed a large increase in permeability of the tissue-tissue interface within 2 hours when we added LPS to the lumen of the upper channel lined by alveolar epithelium in the lung alveolus chip (Fig. 4a). This correlated with disruption of endothelial cell-cell junctions, as demonstrated by immunofluorescence microscopic analysis of VE-cadherin (Fig. 4b,c) and quantitation of the size of the gaps exposed between junctions in the endothelium (Fig. 4c), as well as endothelial activation measured by increased expression of ICAM-1 (Fig. 4d). Importantly, this also correlated with a significant increase in the PBD index in the intact lung chip treated in this manner with LPS and perfused with whole blood, whereas there was no detectable change in platelet-endothelial binding interactions in the absence of the alveolar epithelium (Fig. 4e). Additionally, we observed that large fibrin-containing platelet aggregates appeared in the vascular channel only in intact organ chips containing both the alveolar epithelium and endothelium (Fig. 4f). Furthermore, to confirm that this unique organ-level response to LPS is relevant for pulmonary thrombosis *per se*, we fabricated similar chips using primary human lung microvascular endothelial cells instead of HUVECs in the vascular channel (Fig. S4a). In these studies, addition of LPS to the alveolar epithelium channel produced similar activation of ICAM-1 in the human pulmonary microvascular endothelium within the vascular channel (Fig. S4b,c).

To better characterize this organ-level response to LPS, we took advantage of our ability to collect effluent from the vascular channel of the chips and analyzed cytokine release profiles produced in the lung alveolus-on-a-chip when stimulated with LPS. Of twelve cytokines tested, only three exhibited significant elevation in response to LPS stimulation specifically when the alveolar epithelium was present: interleukin-6 (IL-6), interleukin-8 (IL-8) and monocyte chemotactic protein-1 (MCP-1) (Fig. 4f). Thus, this tissue-tissue interaction that leads to microvascular thrombosis in this model may be mediated at least in part by IL-6 as it has been previously shown to induce ICAM-1 expression in endothelium [39].

Finally, to determine the physiological relevance of these findings, we used our automated imaging technique to analyse the effects of LPS delivered intraperitoneally on platelet-endothelial binding interactions in the mouse cremaster arteriole and vein *in vivo*. Quantitative imaging confirmed that intravenous injection of LPS alone was not sufficient to directly stimulate increased platelet-endothelial binding interactions *in vivo* in both the arteriole and the vein (Fig. S5a,b). In contrast, when these vessels were injured with a laser, thereby releasing inflammatory factors locally, we observed an increase in both platelet-endothelial binding and intravascular thrombus formation (Fig. S5a,b). Taken together, these findings confirm that induction of intravascular pulmonary thrombosis by LPS involves tissue-tissue interactions between the lung alveolar epithelium and vascular endothelium that lead to activation of a cytokine cascade generated by the epithelium which induces the endothelium to become prothrombotic, as suggested by our alveolus chip studies. This

insight into the role of epithelium in vascular inflammation-led alveolar thrombus formation could not have easily been made using *in vivo* animal models or human clinical studies.

Testing of potential antithrombotic therapeutic in the human lung alveolus chip

To further explore the potential value of this model as a preclinical drug development tool, we used the primary lung alveolus chip to analyze the anti-thrombotic and anti-inflammatory activities of a potential drug candidate. Protease activated receptor-1 (PAR-1) has been shown to mediate tissue inflammation and hemostasis, and therefore, it represents a potential target for the treatment of various pathologies leading to coagulation abnormalities, such as, sepsis [40]. Here, we analyzed the effects of parmodulin-2 (PM2), which is a potent PAR-1 inhibitor that has been recently shown to have antithrombotic and vascular protective effects comparable to those of activated protein C (APC) when tested in both a bioengineered endothelium-lined vessel *in vitro* and a recently developed mouse model [41].

In platelets, PAR-1 mediated signaling is critical for platelet activation [42]. Not surprisingly, when we pre-incubated human whole blood with PM2 (30 μM) for 30 minutes before perfusing it through the vascular channel of a LPS-treated alveolus chip, we observed a significant reduction in platelet-endothelial binding in comparison to untreated blood (Fig. 5a). Interestingly, when we first incubated the endothelium-lined vascular channel of the lung chip with PM2 for 4 hours before adding LPS to the alveolar lumen and then perfused human whole blood through the endothelial channel, we found that PM2 treatment of the endothelium significantly decreased thrombi formation (Fig. 5a) as well as pulmonary vascular leakage (Fig. 5b) induced by LPS. Furthermore, preincubation of both the endothelium (4 hours) and blood (30 minutes) with PM2 completely inhibited platelet binding to the endothelium and thrombus formation in the LPS-stimulated alveolus chip (Fig. 5a). Together, these studies with our model indicate that PM2 exhibits potent cytoprotective, as well as anti-thrombotic, activities in human acute lung dysfunction.

To validate the physiological relevance of these results, we carried out similar studies in an *in vivo* model of LPS-induced lung injury [43]. Intratracheal delivery of LPS (1 μg/mouse) to the airway and alveolar epithelium of a mouse (Fig. S6a) resulted in a dose-dependent increase vascular barrier disruption *in vivo* (Fig. S6b). Notably, intravenous administration of the same dose of PM2 as used in our *in vitro* studies (30 μM) significantly reduced the LPS-induced injury of the alveolar tissue *in vivo*, as indicated by a significant improvement of vascular permeability (Fig. S6c), thus confirming the findings we obtained using the lung alveolus chip (Fig. S6b).

DISCUSSION

These studies demonstrate that the primary human lung alveolus chip permits visualization and quantitative real-time analysis of organ-level interactions relevant to *in situ* thrombus formation in human lung. This organ chip technology allowed us to dissect contributions of various human cell types and tissues (epithelium, endothelium and platelets), pro-inflammatory signals (TNF-α and LPS), and fluid flow, as well as a potential antithrombotic and anti-inflammatory therapeutic (PM2), which would be nearly impossible to perform *in vivo*. Thus, this new *in vitro* model of human pulmonary thrombosis offers unique

capabilities that may prove useful for drug development as well as analysis of the pathophysiology of thrombotic diseases.

While it has been recognized that whole blood rheology, mechanics and cellular composition impact vascular biology, immune function, platelet function and signaling pathways involved in hemostasis [44–46], most contemporary *in vitro* analytical devices have not incorporated native whole blood flow in their assessment due to technical difficulties [24,47–50]. A salient feature of the pulmonary organ chip microfluidic system presented here is that it is able to perfuse human whole blood in its native state (recalcified after anticoagulation in sodium citrate) at any desirable shear rate, thereby providing a more physiologically relevant *in vitro* platform to study and analyze intravascular thromboinflammation in the lung. Secondly, by harnessing the potential of modern automated fluorescence microscopy and mathematical modeling, we developed a new way to assess platelet-surface interactions over large spatiotemporal scales. Our analysis shows that the integrated interplay between platelets, thrombi, the vessel wall, and blood flow dynamics can be analyzed in this integrated system-level assay. Significantly, we showed that the pulmonary thrombus formation caused due to endothelial activation in this *in vitro* model correlates well with thrombosis that occurs *in vivo* in response to laser injury in mice, both in terms of morphology and regional heterogeneity, and well as platelet binding dynamics [31,36].

By incorporating primary human alveolar epithelial cells in this modified system, we overcame a limitation of the previously described lung chip that used a human lung tumor-derived alveolar epithelial cell line [20,21], which could exhibit pro-thrombotic activities and thereby complicate studies involving inflammatory activation. The co-culture of this primary alveolar epithelium with human vascular endothelium inside the alveolus-chip for up to 2 weeks allowed us to highlight the critical role that alveolar epithelium plays in pulmonary thrombosis induced by LPS endotoxin. The finding that the presence of LPS in lung does not promote thrombosis by acting directly on the endothelium would be very difficult to show *in vivo* in real-time, as individual tissue and cellular compartments inside the organ cannot be regulated separately, and blood flow inside the lung vessels cannot be controlled or observed over large areas as we can do using the organ chip technology.

However, the full potential of the current model has not yet been explored. For example, in the present study, we did not mimic lung breathing motions which were previously shown to have important effects on lung physiology (e.g., surfactant production, absorption of nanoparticulates, induction of pulmonary edema by interleukin-2) [20,21], and which also could potentially influence pulmonary thrombosis. Another potential caveat is that we used HUVECs, and not lung-specific endothelial cells, in most of our studies; however, when we replaced them with primary human microvascular endothelial cells in our LPS stimulation experiments, we obtained nearly identical results and similar findings were reported using HUVECs and lung microvascular endothelium in prior lung chip studies[20]. We did not analyze the role of immune cells (e.g, neutrophils) in this study for simplicity and to accommodate high-speed imaging with fewer fluorescent channels, but this could be done in future studies as shown in past work with the human organ chips[19,20].

Nevertheless, this primary human lung alveolus chip methodology allowed us to recapitulate many features of vascular thrombosis *in vitro* that have only previously been observed *in vivo*. Notably, we were able to dissect the significance of alveolar epithelium in the onset and propagation of platelet function and thrombosis in acute lung injury. It also allowed us to unravel the cytoprotective and anti-thrombotic effects of a novel PAR-1 antagonist in the setting of acute lung injury and whole blood perfusion. Thus, this human pulmonary alveolar chip model may offer a new tool for pre-clinical testing of antithrombotic drugs that can potentially detect their unwanted thrombotic side effects before they enter human clinical trials. This system also can be used to study fundamental mechanisms of hemostasis regulation in a more physiologically relevant organ-level context. Finally, this tool could offer a new method for a personalized assessment of drug responses to therapy, as well as potential toxicities, by obtaining lung cells (e.g, from biopsies or using lung cells differentiated from induced pluripotent stem cells) and blood from the same patient, and thereby help to individualize therapeutic regimens in the future.

METHODS

Materials and Methods are available in Supplementary Information

Supplementary Material

Refer to Web version on PubMed Central for supplementary material.

Acknowledgments

We thank R. Novak, B. Boettner, J. Fraser, D. Conegliano, S. Denagamage, T. Ferrante, M. Ingram, A. Vernet and G. Merrill-Skoloff for their helpful input and technical support. This work was funded by DARPA contract N66001-11-1-4180, HR0011-13-C-0025, Janssen Pharmaceuticals and the Wyss Institute for Biologically Inspired Engineering at Harvard University.

NIH Grant R01 EB02004-01

References

1. Glas GJ, et al. Bronchoalveolar hemostasis in lung injury and acute respiratory distress syndrome. J. Thromb. Haemost. 2013; 11:17–25. [PubMed: 23114008]
2. Wygrecka M, Jablonska E, Guenther A, Preissner KT, Markart P. Current view on alveolar coagulation and fibrinolysis in acute inflammatory and chronic interstitial lung diseases. Thromb. Haemost. 2008; 99:494–501. [PubMed: 18327397]
3. Bozza FA, Shah AM, Weyrich AS, Zimmerman GA. Amicus or Adversary: Platelets in Lung Biology, Acute Injury, and Inflammation. Am. J. Respir. Cell Mol. Biol. 2009; 40:123–134. [PubMed: 18723438]
4. Finigan JH. The coagulation system and pulmonary endothelial function in acute lung injury. Microvasc. Res. 2009; 77:35–38. [PubMed: 18938186]
5. Cuttica MJ, Machado R. Pulmonary artery thrombosis: another piece to the acute chest syndrome puzzle. Am. J. Respir. Crit. Care Med. 2011; 184:990–991. [PubMed: 22045743]
6. Herve P, et al. Pathobiology of pulmonary hypertension. The role of platelets and thrombosis. Clin. Chest Med. 2001; 22:451–458. [PubMed: 11590840]
7. Toshner* M, Pepke-Zaba* J. Chronic thromboembolic pulmonary hypertension: time for research in pathophysiology to catch up with developments in treatment. F1000Prime Rep. 2014; 6

8. Matute-Bello G, Frevert CW, Martin TR. Animal models of acute lung injury. Am. J. Physiol. - Lung Cell. Mol. Physiol. 2008; 295:L379–L399. [PubMed: 18621912]
9. Vivero M, Padera RF. Histopathology of Lung Disease in the Connective Tissue Diseases. Rheum. Dis. Clin. N. Am. 2015; 41:197–211.
10. Johnson SR, Granton JT, Mehta S. Thrombotic arteriopathy and anticoagulation in pulmonary hypertension. Chest. 2006; 130:545–552. [PubMed: 16899857]
11. Benam KH, et al. Engineered in vitro disease models. Annu. Rev. Pathol. 2015; 10:195–262. [PubMed: 25621660]
12. Bhatia SN, Ingber DE. Microfluidic organs-on-chips. Nat. Biotechnol. 2014; 32:760–772. [PubMed: 25093883]
13. Jackson SP. The growing complexity of platelet aggregation. Blood. 2007; 109:5087–5095. [PubMed: 17311994]
14. Sagripanti A, Carpi A. Antithrombotic and prothrombotic activities of the vascular endothelium. Biomed. Pharmacother. 2000; 54:107–111. [PubMed: 10759296]
15. Wolberg AS, Aleman MM, Leiderman K, Machlus KR. Procoagulant activity in hemostasis and thrombosis: Virchow's triad revisited. Anesth. Analg. 2012; 114:275–285. [PubMed: 22104070]
16. Andrews DA, Low PS. Role of red blood cells in thrombosis. Curr. Opin. Hematol. 1999; 6:76. [PubMed: 10088636]
17. Weyrich AS, Zimmerman GA. Platelets in lung biology. Annu. Rev. Physiol. 2013; 75:569–591. [PubMed: 23043249]
18. Casa LD, Deaton DH, Ku DN. Role of high shear rate in thrombosis. J. Vasc. Surg. 2015; 61:1068–1080. [PubMed: 25704412]
19. Ingber DE. Reverse Engineering Human Pathophysiology with Organs-on-Chips. Cell. 2016; 164:1105–1109. [PubMed: 26967278]
20. Huh D, et al. Reconstituting Organ-Level Lung Functions on a Chip. Science. 2010; 328:1662–1668. [PubMed: 20576885]
21. Huh D, et al. A Human Disease Model of Drug Toxicity-Induced Pulmonary Edema in a Lung-on-a-Chip Microdevice. Sci. Transl. Med. 2012; 4:159ra147.
22. Lieber M, Smith B, Szakal A, Nelson-Rees W, Todaro G. A continuous tumor-cell line from a human lung carcinoma with properties of type II alveolar epithelial cells. Int. J. Cancer. 1976; 17:62–70. [PubMed: 175022]
23. Benam KH, et al. Small airway-on-a-chip enables analysis of human lung inflammation and drug responses in vitro. Nat. Methods. 2015; doi: 10.1038/nmeth.3697
24. Colace T, Falls E, Zheng XL, Diamond SL. Analysis of morphology of platelet aggregates formed on collagen under laminar blood flow. Ann. Biomed. Eng. 2011; 39:922–929. [PubMed: 20949319]
25. Neeves KB, et al. Sources of variability in platelet accumulation on type 1 fibrillar collagen in microfluidic flow assays. PloS One. 2013; 8:e54680. [PubMed: 23355889]
26. Cosemans JM, Angelillo-Scherrer A, Mattheij NJ, Heemskerk JW. The effects of arterial flow on platelet activation, thrombus growth, and stabilization. Cardiovasc. Res. 2013; 99:342–352. [PubMed: 23667186]
27. Pircher J, et al. Prothrombotic effects of tumor necrosis factor alpha in vivo are amplified by the absence of TNF-alpha receptor subtype 1 and require TNF-alpha receptor subtype 2. Arthritis Res. Ther. 2012; 14:R225. [PubMed: 23079185]
28. Jain A, et al. Assessment of whole blood thrombosis in a microfluidic device lined by fixed human endothelium. Biomed. Microdevices. 2016; 18:73. [PubMed: 27464497]
29. Furie B, Furie BC. Mechanisms of thrombus formation. N. Engl. J. Med. 2008; 359:938–949. [PubMed: 18753650]
30. Cooley BC. In vivo fluorescence imaging of large-vessel thrombosis in mice. Arterioscler. Thromb. Vasc. Biol. 2011; 31:1351–1356. [PubMed: 21393581]
31. Stalker TJ, et al. A systems approach to hemostasis: 3. Thrombus consolidation regulates intrathrombus solute transport and local thrombin activity. Blood. 2014; 124:1824–1831. [PubMed: 24951426]

32. Falati S, Gross P, Merrill-Skoloff G, Furie BC, Furie B. Real-time in vivo imaging of platelets, tissue factor and fibrin during arterial thrombus formation in the mouse. Nat. Med. 2002; 8:1175–1181. [PubMed: 12244306]
33. Westein E, Witt S, de Lamers M, Cosemans JM, Heemskerk JW. Monitoring in vitro thrombus formation with novel microfluidic devices. Platelets. 2012; 23:501–509. [PubMed: 22873212]
34. Hansen RR, et al. High content evaluation of shear dependent platelet function in a microfluidic flow assay. Ann. Biomed. Eng. 2013; 41:250–262. [PubMed: 23001359]
35. Jain A, et al. A shear gradient-activated microfluidic device for automated monitoring of whole blood haemostasis and platelet function. Nat. Commun. 2016; 7:10176. [PubMed: 26733371]
36. Welsh JD, et al. A systems approach to hemostasis: 1. The interdependence of thrombus architecture and agonist movements in the gaps between platelets. Blood. 2014; 124:1808–1815. [PubMed: 24951424]
37. Proudfoot AG, McAuley DF, Griffiths MJD, Hind M. Human models of acute lung injury. Dis. Model. Mech. 2011; 4:145–153. [PubMed: 21357760]
38. Liu F, Li W, Pauluhn J, Trübel H, Wang C. Lipopolysaccharide-induced acute lung injury in rats: comparative assessment of intratracheal instillation and aerosol inhalation. Toxicology. 2013; 304:158–166. [PubMed: 23313377]
39. Wung BS, Ni CW, Wang DL. ICAM-1 induction by TNFalpha and IL-6 is mediated by distinct pathways via Rac in endothelial cells. J. Biomed. Sci. 2005; 12:91–101. [PubMed: 15864742]
40. Hawiger J, Veach RA, Zienkiewicz J. New paradigms in sepsis: from prevention to protection of failing microcirculation. J. Thromb. Haemost. 2015; :1743–56. DOI: 10.1111/jth.13061 [PubMed: 26190521]
41. De Ceunynck K, et al. A chemical APC mimetic protects endothelium from thromboinflammatory injury. Rev.
42. Aisiku O, et al. Parmodulins inhibit thrombus formation without inducing endothelial injury caused by vorapaxar. Blood. 2015; 125:1976–1985. [PubMed: 25587041]
43. Conti G, et al. Evaluation of lung inflammation induced by intratracheal administration of LPS in mice: comparison between MRI and histology. Magn. Reson. Mater. Phys. Biol. Med. 2010; 23:93–101.
44. Wootton DM, Ku DN. Fluid mechanics of vascular systems, diseases, and thrombosis. Annu. Rev. Biomed. Eng. 1999; 1:299–329. [PubMed: 11701491]
45. Fogelson AL, Neeves KB. Fluid Mechanics of Blood Clot Formation. Annu. Rev. Fluid Mech. 2015; 47:377–403. [PubMed: 26236058]
46. Flamm MH, Diamond SL. Multiscale systems biology and physics of thrombosis under flow. Ann. Biomed. Eng. 2012; 40:2355–2364. [PubMed: 22460075]
47. Zheng Y, et al. In vitro microvessels for the study of angiogenesis and thrombosis. Proc. Natl. Acad. Sci. U. S. A. 2012; 109:9342–9347. [PubMed: 22645376]
48. Zhang B, Peticone C, Murthy SK, Radisic M. A standalone perfusion platform for drug testing and target validation in micro-vessel networks. Biomicrofluidics. 2013; 7:44125. [PubMed: 24404058]
49. Tsai M, et al. In vitro modeling of the microvascular occlusion and thrombosis that occur in hematologic diseases using microfluidic technology. J. Clin. Invest. 2012; 122:408–418. [PubMed: 22156199]
50. Li X, Xu S, He P, Liu Y. In Vitro Recapitulation of Functional Microvessels for the Study of Endothelial Shear Response, Nitric Oxide and [Ca2+]i. PLOS One. 2015; 10:e0126797. [PubMed: 25965067]

STUDY HIGHLIGHTS

What is the current knowledge on the topic?

Animal models have been used to model the effects of drugs on pulmonary thrombosis, however, they do not mimic the physiology, altered hemostasis or vasculopathies observed in human lung.

What question did this study address?

This study explored whether microfluidic organ-on-a-chip cell culture device can be used to model pulmonary thrombosis at organ level, and measure the effects of drugs on this process.

What this study adds to our knowledge?

This study demonstrates that key elements of human pulmonary thrombosis can be modelled *in vitro* using organs-on-chips. This model showed that LPS endotoxin indirectly stimulates intravascular thrombosis, and inhibitory effects on endothelial activation and thrombosis of a prospective antithrombotic therapeutic can be recapitulated.

How this might change clinical pharmacology or translational science?

This new methodology will enable *in vitro* analysis of human thrombotic responses to potential new therapeutics within the lung microvasculature at the cell, tissue and organ levels, not currently possible with animal models.

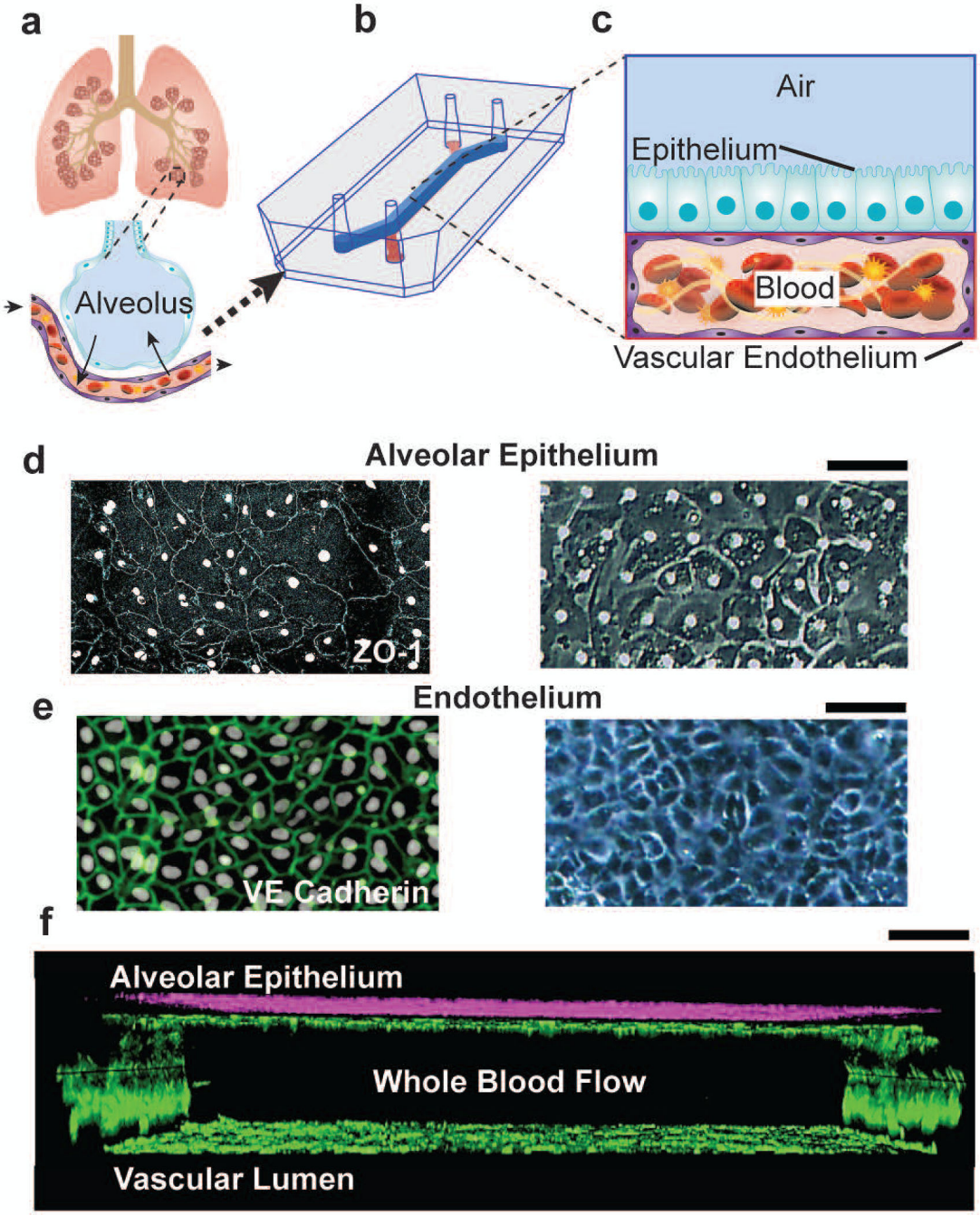

Figure 1. Microengineered model of human pulmonary thrombosis-on-chip

a) A conceptual schematic of the human lung showing that the alveoli interact with the neighboring blood vessels during hemostasis or pulmonary dysfunction. **b**) Engineering drawing of the microdevice containing two PDMS compartments separated by a thin porous membrane that reproduces the microarchitecture of the alveolar-capillary interface. **c**) Graphic illustration showing the top compartment (1 mm wide and 1 mm tall) is cultured with human primary alveolar epithelial cells and the entire bottom chamber (1 mm wide and 250 μm tall) lined with human endothelial cells forming a lumen. Whole blood is perfused

through the bottom chamber and thrombus formation is visualized using fluorescence microscopy from the bottom. **d**) Micrograph of human lung alveolar epithelial cells (ZO1, left; brightfield, right; Scale bar, 50 μm) and **e**) vascular endothelial cells (VE-cadherin, left; brightfield, right, Scale bar, 50 μm) **f)** Sideview of confocal micrographs showing junctional structures, after twelve days of co-culture, of a single layer of the primary alveolar epithelium at the top chamber (purple, stained with E-cadherin) and endothelial monolayers covering the entire surface of the lower chamber (green, stained with VE-cadherin), through which blood perfusion takes place. Scale bar: 100 μm.

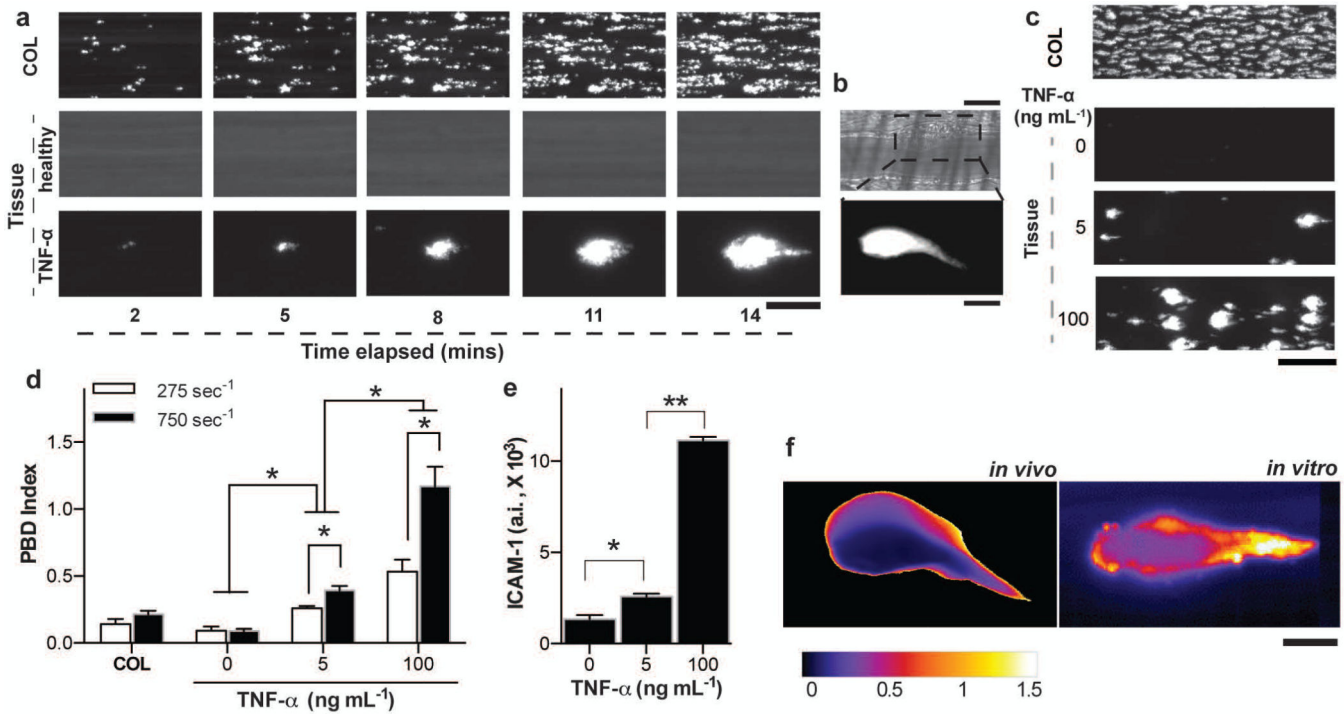

Figure 2. Analysis of dynamical progression of thrombus formation in the alveolus chip

a) Fluorescence micrographs depicting a section of the imaged microchannel (Scale bar, 25 μm) showing platelet accumulation over time (left to right) on collagen (top), a healthy blood vessel (middle), TNF-α stimulated vessel (bottom) and **b)** platelet accumulation after 4 minutes of laser-induced injury on a mouse cremaster arteriole (top, bright field and bottom, fluorescence; Scale bar, 25 μm, top and bottom). **c)** Fluorescent micrographs of a large section of the vascular chamber showing luminal thrombus formation on bare collagen (topmost) and TNF-α stimulated endothelium in a dose dependent manner (bottom three; Scale bar, 100 μm). **d)** Sensitivity analysis of the platelet-endothelial dynamics algorithm (PBD index), showing that in conditions of vascular injury/collagen or healthy endothelium, the dynamical events characterizing clot formation are nearly absent but they increase in a TNF-α dose dependent manner. The PBD index is also sensitive to applied shear rate (n = 3, *P<0.05, 2-way ANOVA). **e)** ICAM-1 expression on the endothelial cells after stimulation of the vessel with TNF-α (n = 4, *P<0.05, unpaired t-test). **f)** Image colormap showing the coefficient of variability (calculated from the fluorescence image timeseries) within a laser-induced thrombus *in vivo* (left) and TNF-α induced thrombus on a vsacular lumen *in vitro* (right). Scale bar, 20 μm.

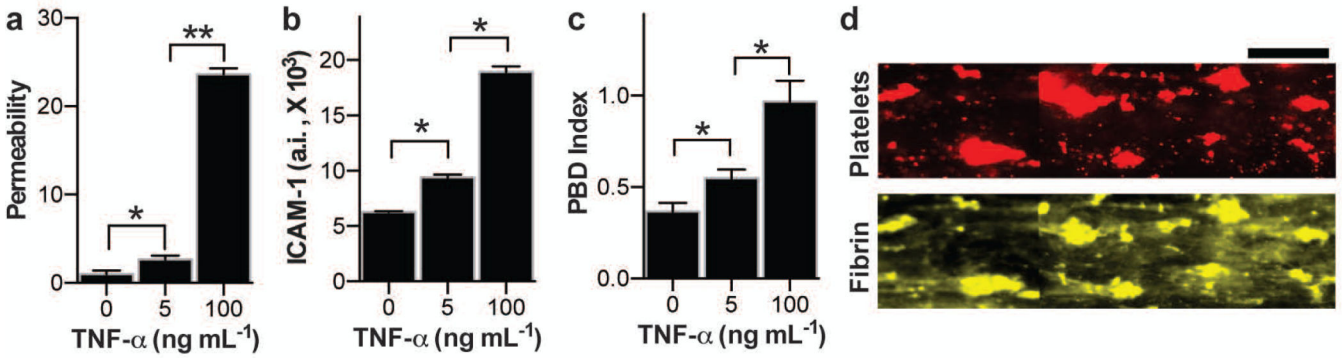

Figure 3. TNF-α induced endothelial disruption and thrombus formation in alveolus chip

Inside the lung alveolus-on-a-chip that was either left untreated (0 ng mL^{-1}) or treated with 5 or 100 ng mL^{-1} of TNF-α, **a)** measurement of vascular permeability (fluorescence normalized by untreated vascular tissue; n=4), **b)** vascular ICAM-1 measured on the vascular surface (n=4), and **c)** measurement of PBD index after whole blood perfusion (n=3). **a–c**, *P<0.05, **P<0.01, 1-way ANOVA. **d)** Representative fluorescence micrographs showing platelet aggregates (red) and fibrin (yellow) at the end of blood perfusion through the alveolus-chip after TNF-α stimulation (Scale bar, 100 μm).

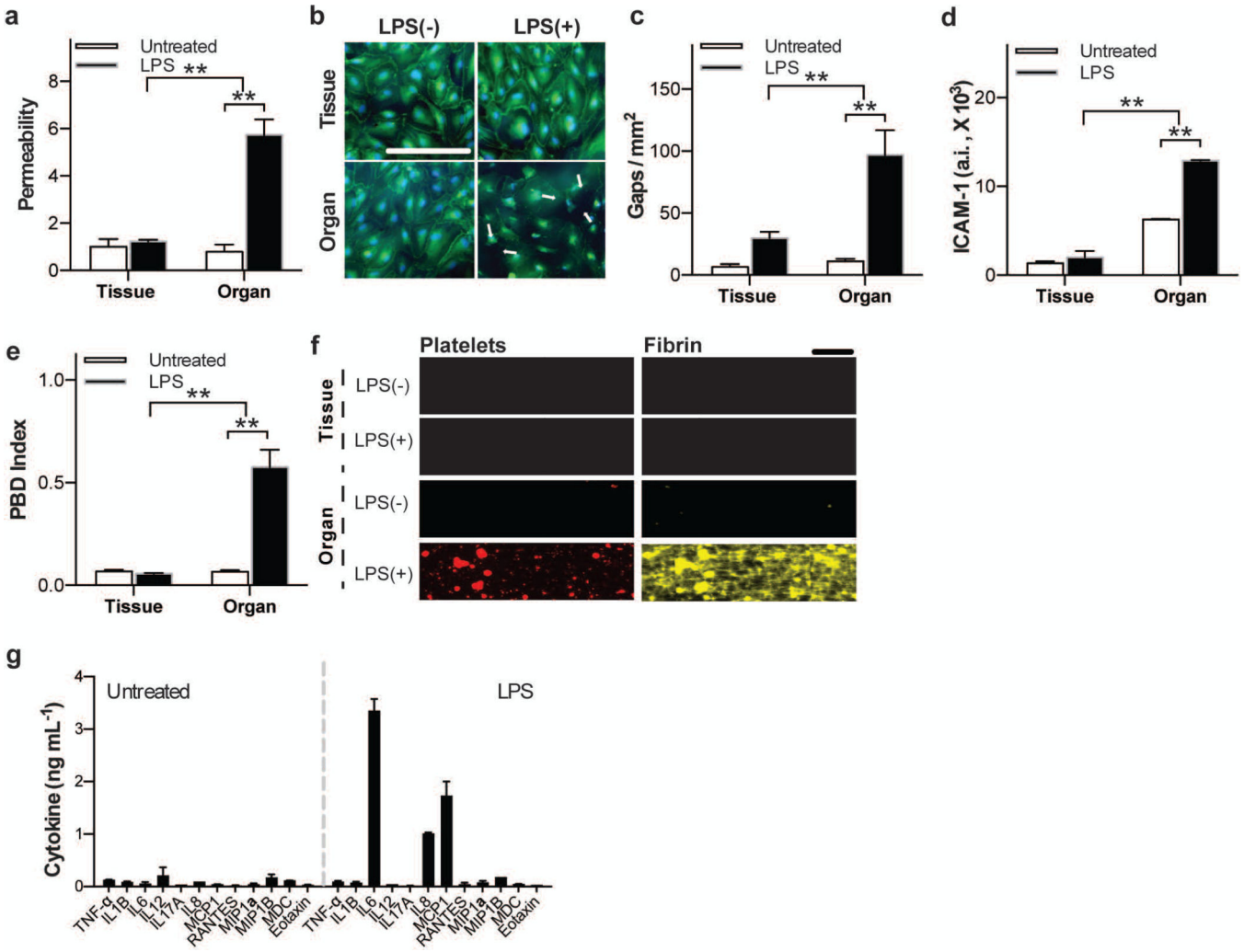

Figure 4. LPS-induced endothelial disruption and thrombus formation when LPS was added to the vascular channel of a chip lined only by vascular endothelium or to the epithelial channel of an intact lung alveolus chip

a) Vascular permeability measurements (fluorescence normalized by untreated vascular tissue; n=4) demonstrate that LPS only compromised barrier function when presented to the epithelium in an organ-level context. **b)** Representative confocal micrographs showing that VE cadherin-labeled endothelial cell-cell adhesions (green) open and retract when LPS was added to the chip containing both the epithelium and endothelium in an organ context (Organ), but not when added directly to the endothelium alone (tissue) (bar, 100 μm; arrows indicate gaps; blue, DAPI-stained nuclei). **c)** Quantification of averaged gap areas resulting from discontinuous VE-cadherin staining, as shown in **b** (n=4).**d)** Quantification of vascular ICAM-1 on the endothelial cell surface under the conditions shown in **b** (n=4). **e)** Measurement of PBD indices after whole blood perfusion through the control and LPS-treated lung alveolus chips (n=3). **f)** Representative fluorescence micrographs showing platelet aggregates and fibrin within the vascular channel at the end of blood perfusion through the alveolus chip (bar, 100 μm;**a,c,d,e** *P<0.05, **P<0.01, 2-way ANOVA). **g)** Quantification of cytokines released, as measured within the effluent of the vascular channel,

showing significant differences in a subset of cytokines following 2h of LPS stimulation compared to untreated conditions (n=2).

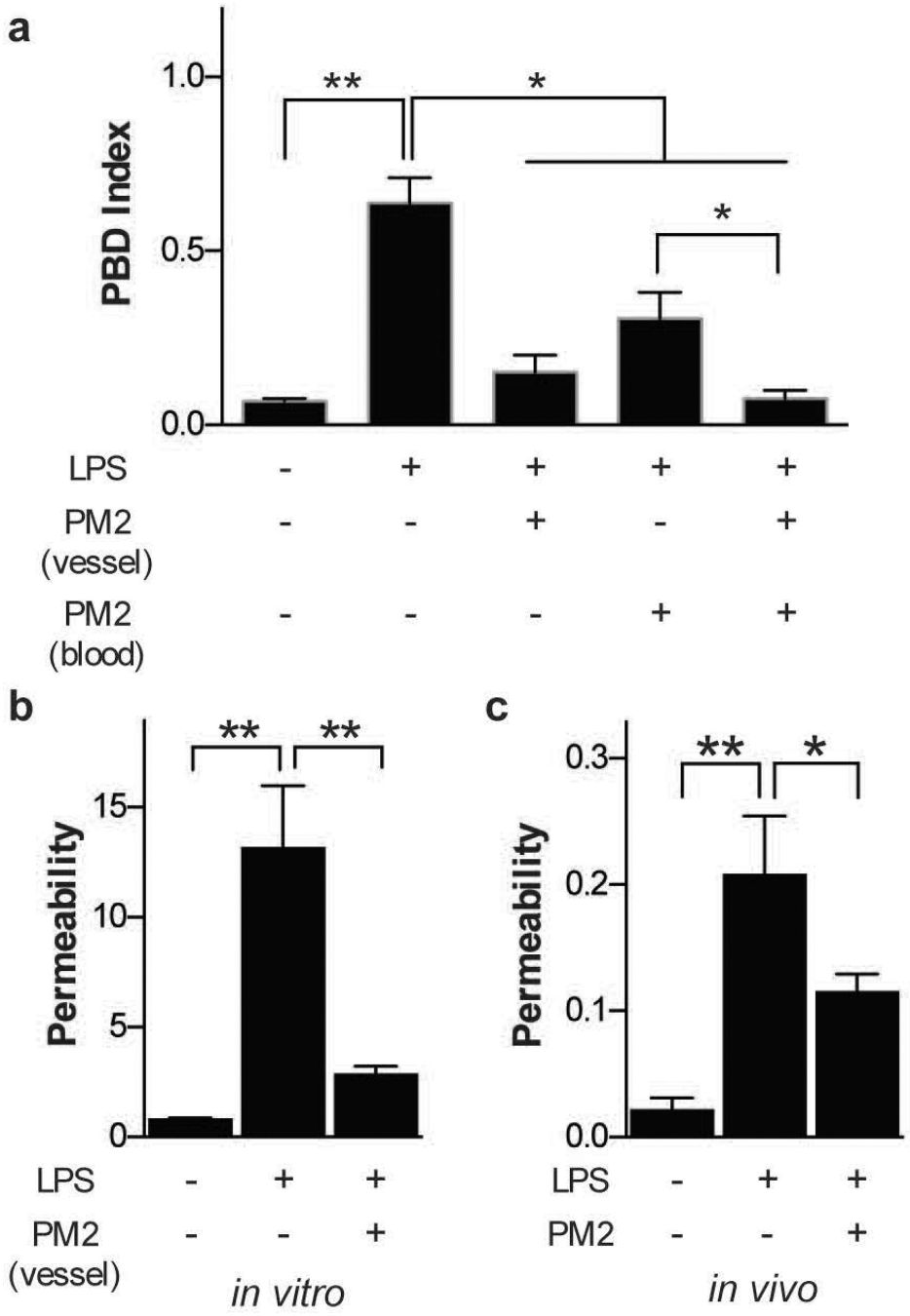

Figure 5. Therapeutic effect of a PAR-1 inhibitor (*parmodulin*) in lung injury

a) PBD index measured in the chip after blood perfusion through the vascular channel of an alveolus chip previously exposed to LPS (100 ng mL^{-1} for 2 hours) on the epithelial side, while the blood, the endothelium or both were treated with parmodulin (PM2) before perfusion. **b**) Vascular permeability (fluorescence normalized by untreated vascular tissue) measured inside the LPS-treated microdevice with or without treatment of parmodulin 2. **c)** Vascular permeability measurements *in vivo* after intratracheal delivery of LPS (1 μg per

mouse) for 2 hours and systemic delivery of parmodulin (PM2, 30 μM) for 4 hours (**a-c**, n=3. *P<0.05, **P<0.01, 1-way ANOVA).